



## Self-Healing and Shape-Memory Hydrogels

### Kendini Onarabilen ve Şekil-Hafızalı Hidrojeller

Oguz Okay<sup>✉</sup>

Department of Chemistry, Istanbul Technical University, Maslak, Istanbul, Turkey.

#### ABSTRACT

Hydrogels are soft and smart materials with great similarity to biological systems. In the past decade, a significant progress has been achieved to produce mechanically strong and tough hydrogels. Another major challenge in gel science is to generate self-healing and shape-memory functions in hydrogels to extend their application areas. Several strategies have been developed to create self-healing ability in hydrogels by replacing the chemically cross-linked polymer network with a reversible one. Moreover, a combination of strong and weak physical cross-links was used to produce hydrogels with both self-healing and shape-memory behavior. In this review, I present recent developments in the field of self-healing and shape memory hydrogels by mainly focusing our achievements.

#### Key Words

Hydrogels, self-healing, shape-memory.

#### ÖZ

Biyolojik sistemlere büyük bir benzerlik gösteren hidrojeller yumuşak ve akıllı malzemelerdir. Mekanik olarak dayanıklı ve tok hidrojellerin üretimi konusunda geçen on yılda önemli ilerlemeler sağlanmıştır. Jel biliminde mevcut diğer büyük zorluk ise hidrojellerin kullanım ömürlerinin uzatılması için onlara kendini onarım ve şekil-hafıza fonksiyonlarının kazandırılmasıdır. Bu derlemede, kendini onarabilen ve şekil-hafızalı hidrojeller alanında son gelişmeleri sunuyorum.

#### Anahtar Kelimeler

Hidrojeller, kendini onarma, şekil-hafıza.

**Article History:** Received: Sep 20, 2020; Revised: Sep 20, 2020; Accepted: Oct 20, 2020; Available Online: Oct 20, 2020.

**DOI:** <https://doi.org/10.15671/hjbc.797525>

**Correspondence to:** O. Okay, Department of Chemistry, Istanbul Technical University, Maslak, Istanbul, Turkey.

**E-Mail:** okayo@itu.edu.tr

## INTRODUCTION

Hydrogels are physically or chemically cross-linked hydrophilic polymer chains containing water without dissolving [1]. Softness, stimuli-responsiveness, and great similarity to biological systems make hydrogels unique materials for a wide range of applications including in biomedical and tissue engineering, sensors, artificial organs, and actuators [2,3]. After the pioneering works of Wichterle on the biomedical application of hydrogels [4], and Tanaka on smart hydrogels [5], the number of publications on hydrogels has increased rapidly (Figure 1a). However, we should note that the history of gel science traces back to the time of Staudinger. In 1935, Staudinger and Heuer were the first to show that the presence of a small amount of divinylbenzene cross-linker (around 0.02 wt%) present in styrene leads to the formation of highly swollen gels [6]. Figure 1b shows the first published images of a chemically cross-linked polystyrene gel before (up) and after swelling in benzene (down) [6]. This work can be considered as one of the pioneers of gel science.

The classical first-generation hydrogels have generally been prepared by free-radical cross-linking copolymerization of hydrophilic vinyl and divinyl monomers, or by chemical cross-linking of hydrophilic polymers in aqueous solutions. The main drawback of these hydrogels was their brittle nature and hence weak mechanical properties limiting their load-bearing applications [7]. It was later observed that the mechanical weakness of the classical hydrogels is due to the lack of an effective energy dissipation mechanism within the covalently cross-linked network [7-9]. This lack results in localization of the fracture energy at the point of application of force leading to a fast crack propagation and hence failure at a low strain (Figure 2A). In the past decade, intensive works have been focused on generating an effective energy dissipation in hydrogels via physical bonds to prevent crack propagation even under large strain (Figure 2B) [9].

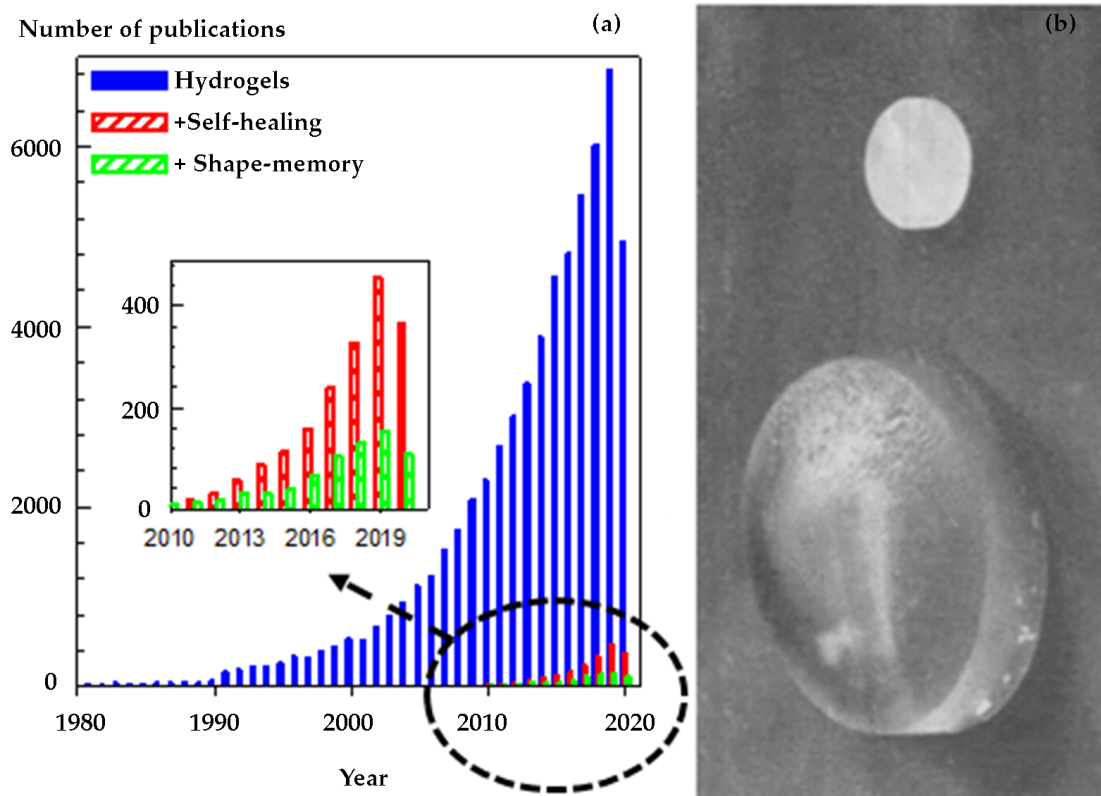


**Figure 1.** (a): The number of papers with keywords “hydrogels”, “hydrogels + self-healing”, and “hydrogels + shape-memory” according to the WoS portal on September 12, 2020. (b): Historical images of a cross-linked polystyrene specimen from 1935 before (up) and after swelling in benzene (down). Reprinted with permission from ref. 6. Copyright 1935. John Wiley and Son.

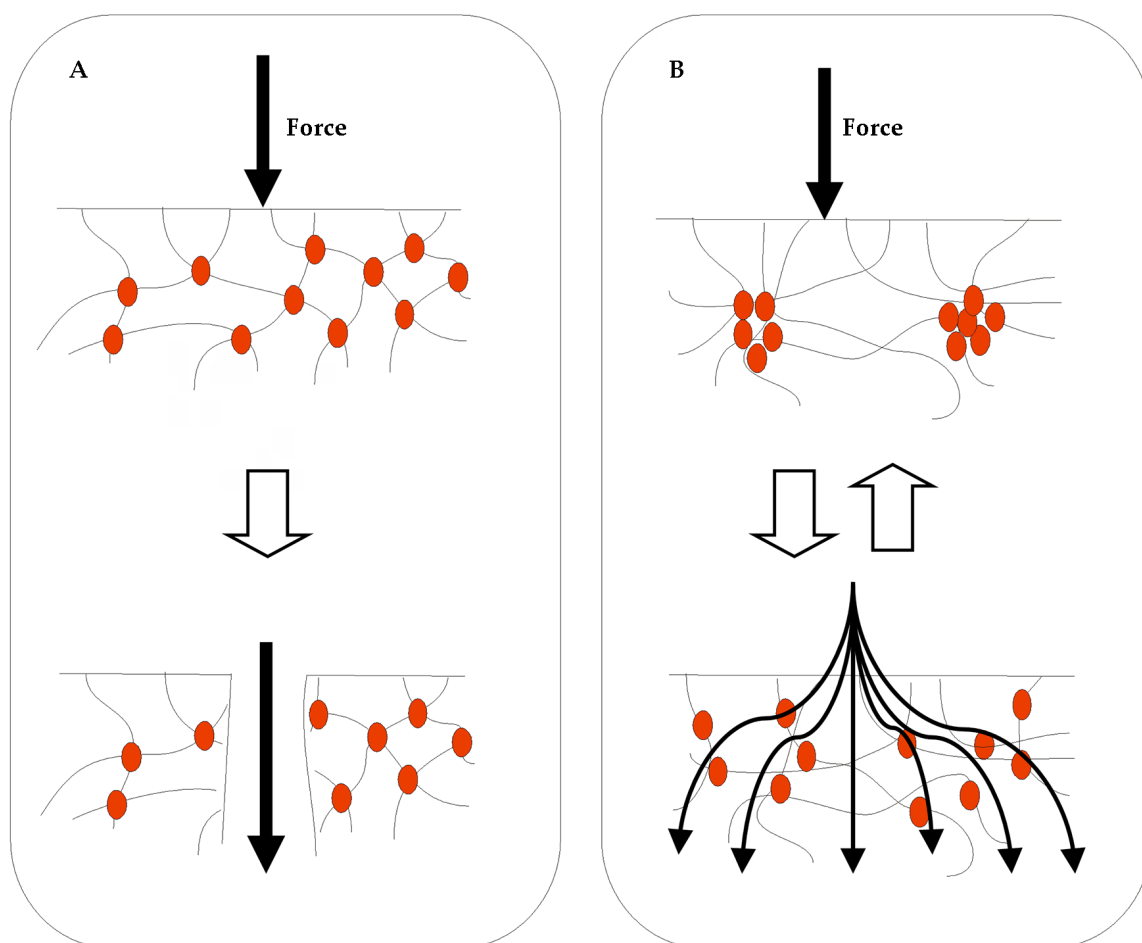


**Figure 2.** Cartoon demonstrating crack of a covalently cross-linked hydrogel due to the localization of the fracture energy (A), and dissipation of the fracture energy in a hydrogel formed by reversible intermolecular bonds (B). Reprinted with permission from ref. 50. Copyright 2009 Elsevier Ltd.

Using the energy dissipation approach, second generation hydrogels have been developed exhibiting extraordinary mechanical performances similar to those of load-bearing tissues, e.g., tendons, cartilage, and ligaments [9-11]. As an example, double-network (DN) hydrogels containing 60-90% water consist of interpenetrated highly cross-linked (brittle) and loosely cross-linked (ductile) polymer networks. Under a low strain, the brittle network component of the DN breaks up to form many cracks by dissipating energy while the ductile component keeps the DN hydrogel together [10]. Figure 3 summarizing recent achievements in terms of the mechanical parameters of second generation hydrogels reveals that they are no more fragile as the classical ones [12-21].

Designing self-healing and shape-memory functions in soft materials is another challenge in the last years, which is the topic of the present review. Self-healing can be defined as the ability of a material to repair its damage autonomously or under external stimuli such as the heat, solvents, light, etc. Self-healing function in synthetic polymers is important as it will extend their lifetimes and reduce the amount of waste polymers including microplastics in the environment. This function is also important for hydrogels in their various application areas such as scaffolds in tissue engineering, biomaterials, and drug delivery systems. Inspired by the natural phenomena observed in blood clotting, or repair of fractured bones, several strategies have been developed recently to create self-healing in polymers and hydrogels [22-30]. Moreover, shape-memory is another capability of a material to remember one or

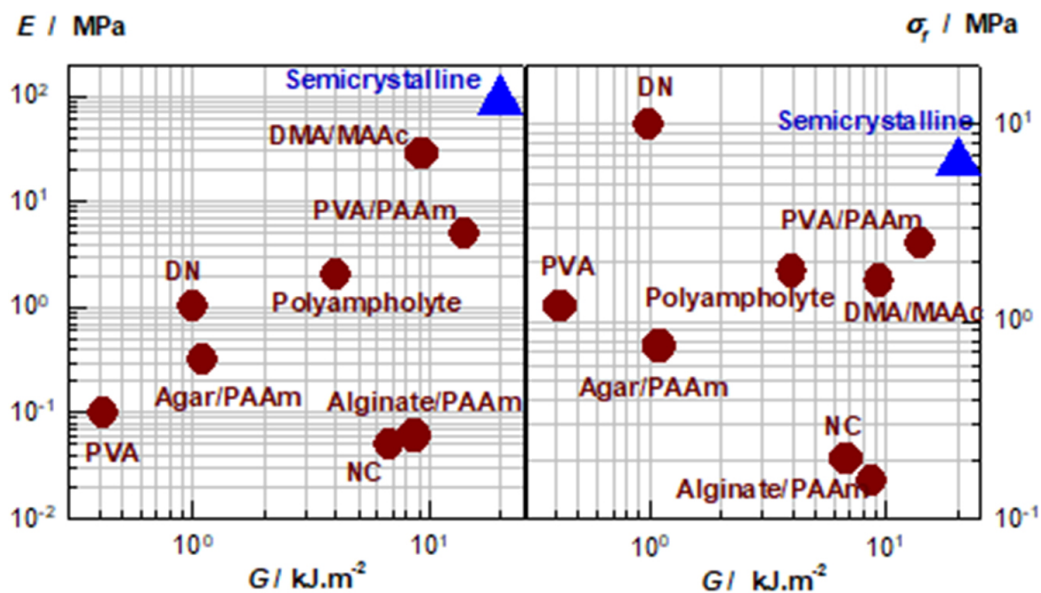


**Figure 3.** The mechanical parameters of second generation hydrogels [12-21].  $E$  = Young's modulus,  $\sigma_t$  = Tensile strength.  $G$  = Fracture energy. The abbreviations are explained in ref. [20]. Reprinted with permission from ref. 20. Copyright 2016 Elsevier Ltd.

more shapes under various stimuli [31-33]. Shape-memory hydrogels have attracted significant interest due to their prime importance as actuators, sensors, and implants for minimally invasive surgery [34-39]. The number of publications on self-healing and shape-me-

memory hydrogels has increased significantly in the past years (inset to Figure 1a). In this review, I present recent developments in the field of self-healing and shape memory hydrogels by mainly focusing our achievements in the past 10 years.

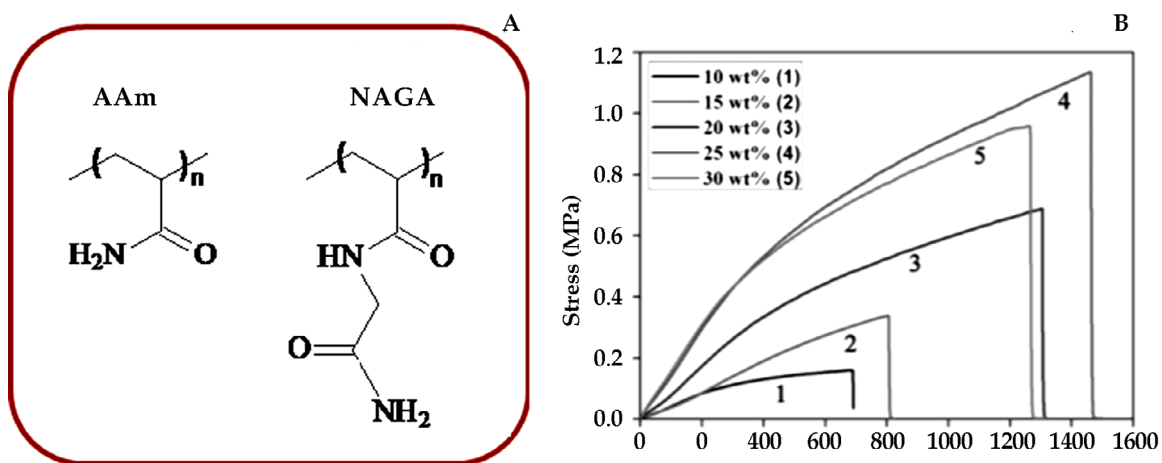


**Figure 4.** (A): Chemical structure of acrylamide (AAM) and N-acryloyl glycinamide (NAGA) segments. (B): Tensile stress-strain curves of NAGA hydrogels. NAGA concentration at the hydrogel preparation is indicated. Figure 4B, from [40] with permission from Wiley.

## 2. Self-healing hydrogels

The self-healing function in hydrogels can be created by replacing the chemical cross-links in their 3D network with physical ones having finite lifetimes. Thus, instead of a chemically cross-linked network with infinite lifetime, a physical polymer network of hydrophilic chains via dynamic covalent bonds or non-covalent interactions is produced. The type and lifetime of the physical bonds are the main factors governing the properties of self-healing hydrogels. Previous works show that self-healing hydrogels prepared by dynamic covalent bonds exhibit poor mechanical properties and their preparation needs complicated synthetic methods [23]. Therefore, this review only covers recent advances in self-healing hydrogels formed via non-covalent interactions by focusing on H-bonding and hydrophobic interactions.

### 2.1 Self-healing via H-bonds

Preparation of physical hydrogels via H-bonds that are stable in water requires multiple H-bonding interactions between polymer chains. For instance, acrylamide (AAm) and N-acryloyl glycinamide (NAGA) are vinyl monomers carrying single and dual amide groups, respectively (Figure 4A) [40]. The free-radical polymerization of 25 w/v% AAm in an aqueous solution leads to the formation of a semidilute polymer solution. This is expected because AAm has a simple amide H-bond and hence, the resulting polymer chains have weak H-bonding interactions so that they dissolve in water. However, replacing AAm with NAGA under the same experimental condition leads to the formation of a hydrogel with a tensile strength in the range of MPa and elongation ratio at break of 1400% (Figure 4B) [40]. Thus, the dual amide H-bonds of NAGA forms mechanically strong H-bonded hydrogels stable in water due to the multiple H-bonding domains. Because NAGA hydrogels have a physically cross-linked network structure, they have self-healing ability with a healing efficiency of 80% induced by heating at 90°C [40]. Temperature-induced healing of NAGA hydrogels occurs due to the dissociation of H-bonds at the elevated temperature so that after cooling to room temperature, H-bonds reform to bridge the damaged surfaces [40].

Diaminotriazine (DAT) groups incorporated into hydrogel network generates H-bonded dimers or higher-order aggregates leading to the formation of mechanically strong H-bonded hydrogels (Figure 5A) [41,42]. Ureidopyrimidinone (UPy) units in the hydrogels can generate UPy-UPy dimers with quadruple H-bonds (Figure 5B) [43]. UPy-

containing hydrogels with 80 wt% water exhibit a tensile strength of 1 MPa, and efficient self-healing properties [43]. Moreover, incorporation of hydrophobic groups in H-bonded hydrogels further increases the H-bond strength and improves their mechanical properties. For instance, Young's modulus of physical 1-vinylimidazole/acrylic acid (AAc) self-healing hydrogels drastically increases when AAc units are replaced with methacrylic acid (MAAc) ones due to their methyl motifs on the backbone. [44,45].

The copolymerization of vinyl monomers with H-bond acceptor and donor sites in aqueous solutions forms self-healing hydrogels with good mechanical properties. For example, MAAc and N,N-dimethylacrylamide (DMAA) have strong H-bond donor carboxylic, and H-bond acceptor carbonyl groups, respectively. Due to the formation of multiple H-bonds between MAAc and DMAA units, their copolymerization in an aqueous solution without a chemical cross-linker leads to self-healing H-bonded hydrogels with a Young's modulus of 28 MPa, and elongation at break of 800% [19].

The cooperativity of H-bonds also affects significantly both the mechanical and self-healing performances of H-bonded hydrogels [46]. To highlight the effect of H-bond cooperativity, one may compare the properties of two hydrogels with identical composition:

- 1) Hydrogel prepared by free-radical copolymerization of AAm and N-vinylpyrrolidone (VP) in an aqueous solution,
- 2) Hydrogel prepared by free-radical polymerization of AAm alone in an aqueous pol(N-vinylpyrrolidone) (PVP) solution.

In both cases, H-bonding interactions occur between the amide and pyrrolidone groups of AAm and PVP, respectively. However, the use of preexisting PVP creates a hydrogel with much higher tensile strength than that formed using the in situ formed PVP [46]. This reveals that the in situ formed PVP generates much weaker H-bonds with polyacrylamide (PAAm) chains as compared to the preexisting PVP. This interesting observation also indicates the importance of so-called proximity effect in H-bonding interactions [46]. Thus, formation of H-bonds between two polymer chains restricts the conformational freedom of the chains, which, in turn, facilitates formation of subsequent H-bonds, the extent of which increases with increasing number of segments in a polymer molecule.

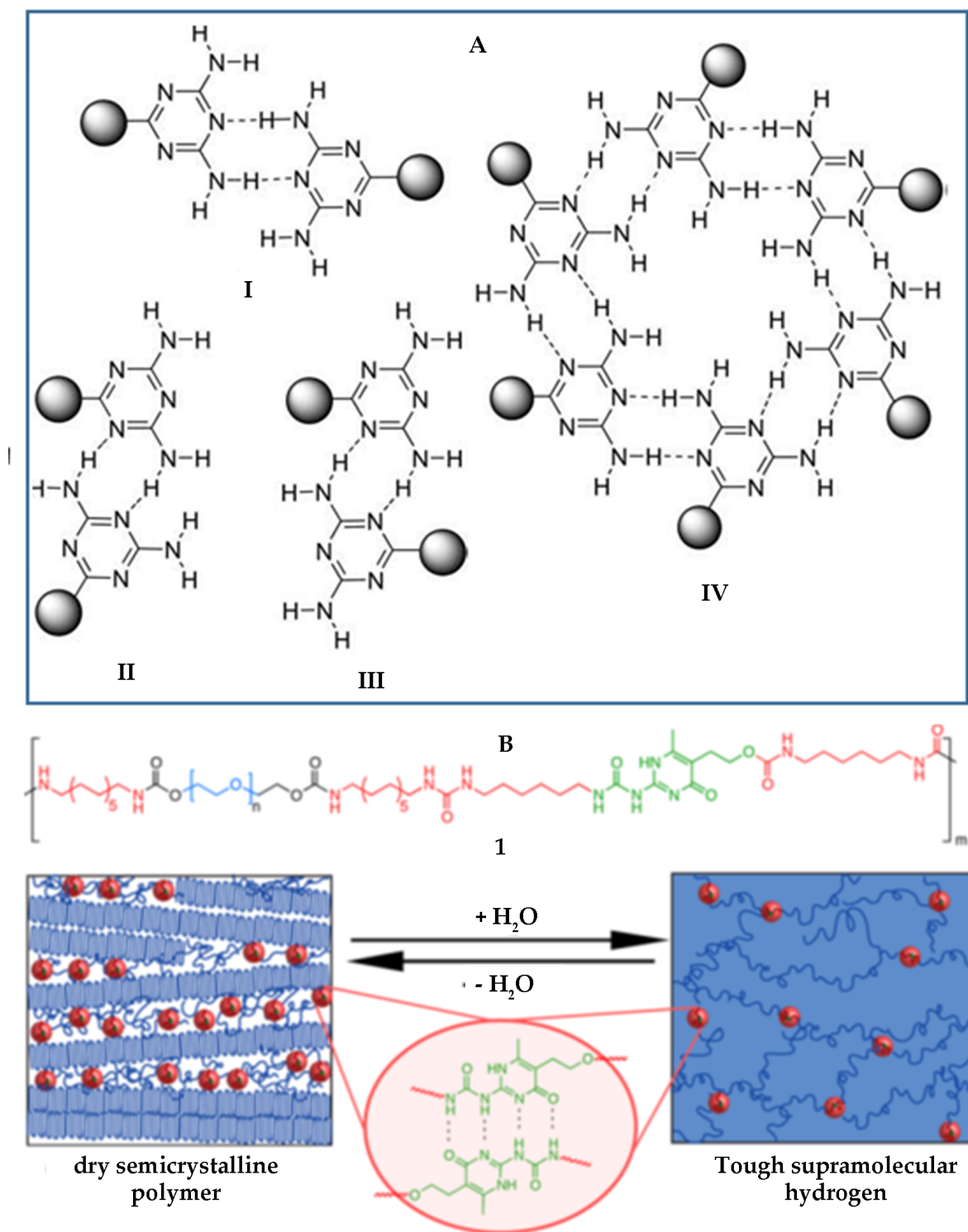


**Figure 5.** (A): Chemical structure of diaminotriazine (DAT) groups. From [41] with permission from the Royal Society of Chemistry. (B): Ureidopyrimidinone (UPy) unit incorporated in a polymer (up), and UPy-UPy dimers with quadruple H-bonds forming a semi-crystalline polymer and hydrogel in dry and wet states, respectively (bottom). From [43] with permission from the American Chemical Society.

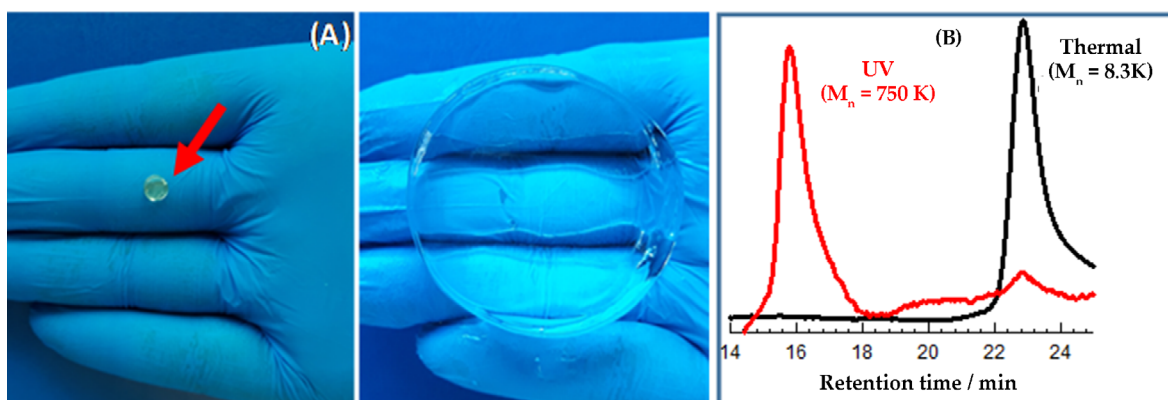


**Figure 6.** (A): Images of a physical PAMPS gel before and after swelling in water. AMPS concentration at the gel preparation is 60 wt% AMPS. (B): GPC traces of linear polymers isolated from the hydrogels using H-bond breaking agent urea (aq). From [47] with permission from the American Chemical Society.

Hydrogels based on 2-acrylamido-2-methyl-1-propanesulfonic acid (AMPS) are attractive soft materials for the preparation of superabsorbent materials. Recently, we observed that UV polymerization of AMPS without a chemical cross-linker produces water-insoluble PAMPS hydrogels with a swelling ratio of  $\sim 1000$  g/g (Figure 6A) [47]. In contrast, PAMPS hydrogels prepared under the same conditions but by thermal polymerization at  $80^{\circ}\text{C}$  are easily soluble in water and exhibit 3-fold lower Young's modulus as compared to those formed by UV polymerization. It was shown that the molecular weight of the primary chains in hydrogels formed by UV polymerization is much larger than that formed by thermal polymerization (Figure 6B) [47]. This finding also highlights significance of the proximity effect in H-bonded hydrogels.

N, N-dimethylacrylamide (DMAA) is a strong H-bond acceptor due to the dimethyl amino groups and hence, can strengthen H-bonds in AMPS hydrogels. It was shown that cross-linker-free copolymerization of AMPS and DMAA in aqueous solutions produces physical hydrogels with a high stretchability (1000%), mechanical strength, and complete self-healing efficiency [47]. When immersed in water, they absorb a large quantity of water without dissolving ( $\sim 1700$  g/g). Calculations reveal that the effective cross-link density of AMPS/DMAA hydrogels significantly increases with increasing DMAA amount in the gel network indicating increasing strength of H-bonds acting as cross-links [47].

Deoxyribonucleic acid (DNA) molecules are carriers of genetic information in their base sequences. DNA hydrogel is a chemically or physically cross-linked net-

work of DNA strands exhibiting their unique characteristics. Self-healable double-stranded (ds) DNA/clay nanocomposite hydrogels were recently prepared by polymerization of DMAA via free-radical mechanism in an aqueous solution of ds-DNA (2000 base pairs) and Laponite nanoparticles [48]. The hydrogels are highly stretchable (1500%) and show thermally induced denaturation and renaturation behavior of ds-DNA. To monitor the conformational transition of ds-DNA in the gel network, DNA/clay hydrogels were prepared in the presence of ethidium bromide (EtBr). EtBr is known to intercalate between the base pairs of DNA, thereby producing a high increase in fluorescence intensity as compared to the single-stranded (ss) DNA. Figure 7A presents this behavior for a DNA/clay hydrogel specimen containing EtBr. EtBr fluorescence spectra are shown during a heating-cooling cycle between 25 and  $90^{\circ}\text{C}$  and the inset presents EtBr emission intensity at 600 nm plotted against the temperature [48]. It is seen that the maximum intensity decreases as the temperature is increased up to  $90^{\circ}\text{C}$  reflecting the conformational transition from double- to single-stranded DNA within the gel network. Upon cooling back to  $25^{\circ}\text{C}$ , EtBr intensity in the gel again increases and rises above its initial value.

The optical photographs of a gel specimen under UV light also visualize this conformational transition between ds- and ss-DNA in the hydrogels (Figure 7B). The initial yellow-orange color of the gel specimen under UV light becomes weaker at  $90^{\circ}\text{C}$  due to the decrease of fluorescence intensity while the initial color is recovered upon cooling to  $25^{\circ}\text{C}$ . Thus, ds-DNA molecules retain their characteristic features within the hydrogel

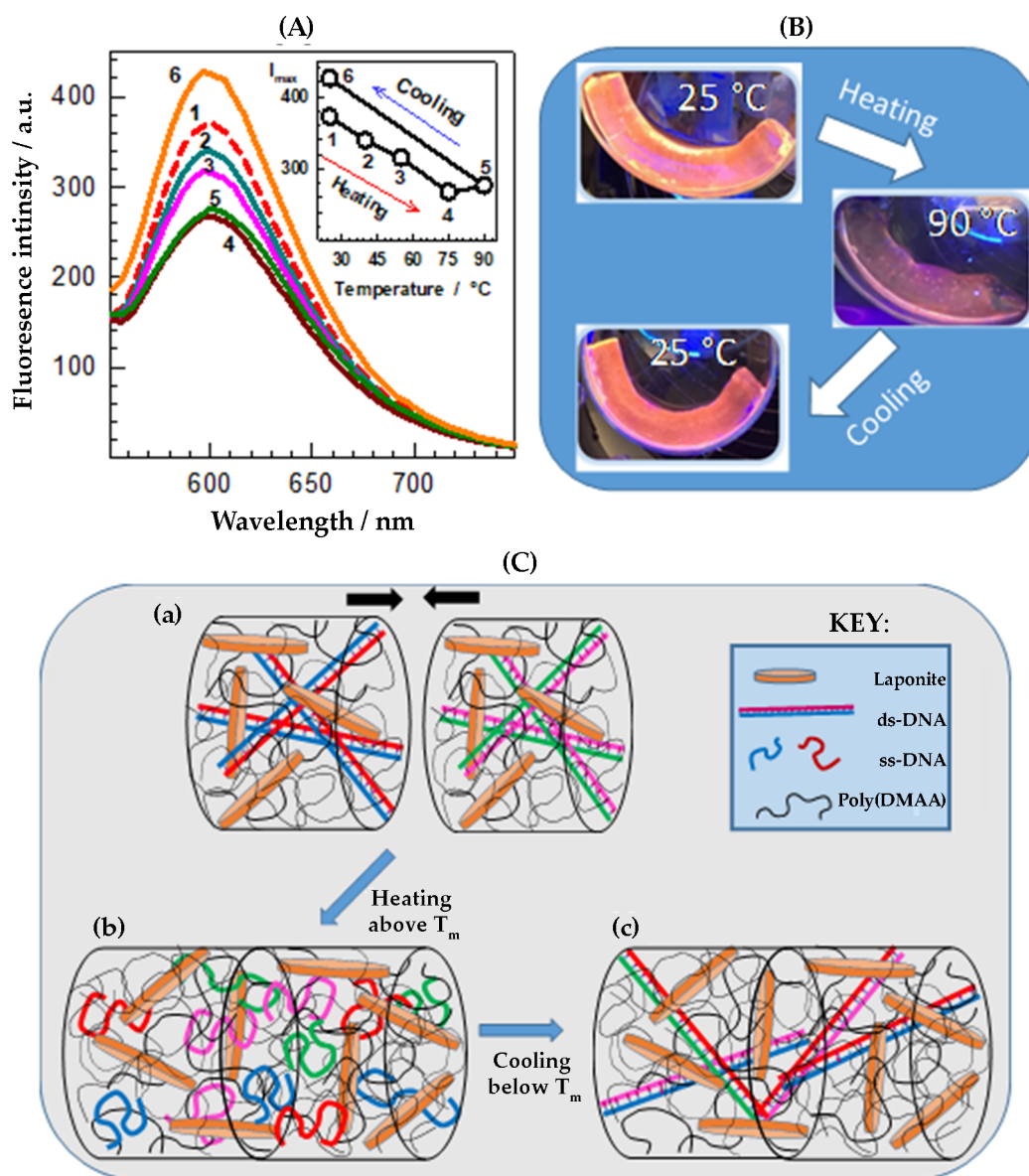


**Figure 7.** (A): EtBr fluorescence spectra in a DNA/clay hydrogel at 25 (1), 40 (2), 55 (3), 75 (4), and 90°C (5), and after cooling back to 25°C (6). The inset shows EtBr emission intensity plotted against the temperature. (B): Images of a DNA/clay hydrogel swollen in 10  $\mu$ M EtBr solution. They were taken under UV light at 25 and 90°C, and after cooling back to 25°C. (C): Cartoon showing cut surfaces of DNA/clay hydrogels (a), and after bringing them together at above (b), and below  $T_m$  of ds-DNA (c). From [48] with permission from the American Chemical Society.

network. DNA/clay hydrogels also exhibit a complete healing efficiency when heated at 90°C for 30 min. The healing mechanism was explained as follows [48]: During heating, H-bonds holding the double strands together weaken and finally break to form flexible ss-DNA strands within the hydrogel network. Upon cooling, the released single strands at the cut region combine to form ds-DNA bridges providing healing of the hydrogels (Figure 7C).

## 2.2 Self-healing via hydrophobic interactions

Hydrogels formed via hydrophobic interactions and/or crystalline domains have been investigated in our research group in the past 20 years [24,25]. For the preparation of such hydrogels containing hydrophilic and hydrophobic regions, micellar polymerization technique has mainly been used. This technique provides copolymerization of water-soluble and water-insoluble monomers in an aqueous solution of surfactant micelles [49-51]. Thus, a hydrophobic monomer is first solubilized within micelles, and then it is copolymerized with a hydrophilic monomer in aqueous solution by a free-radical mechanism (Figure 8). A particular advantage of this approach is the blocky structure of the resulting

polymers significantly enhancing their associative properties.

Thus, instead of a chemical cross-linker, a hydrophobic monomer is incorporated into hydrophilic polymer chains to create hydrophobic associations acting as reversible cross-links. Figure 9A compares the effect of the “physical cross-linker” dodecyl methacrylate (C12M) with that of the chemical cross-linker N'-methylenebis(acrylamide) (BAAM) [51]. The storage modulus  $G'$  (symbols) and the loss factor  $\tan \delta$  (lines) of the reaction system are plotted against the reaction time during the micellar copolymerization of acrylamide (AAM) and 1 mol% C12M or BAAM. The limiting value of the storage modulus  $G'$  at long reaction times does not change much depending on the type of the cross-linker revealing that the cross-link density of both hydrogels remains almost unchanged. However, C12M segments incorporated into the PAAm network generate a hydrogel with a much higher  $\tan \delta$  as compared to that formed using the classical chemical cross-linker BAAM. This reveals the reversible nature of C12M associations (cross-links) due to the dissociation and re-association of the dodecyl side chains within the expe-

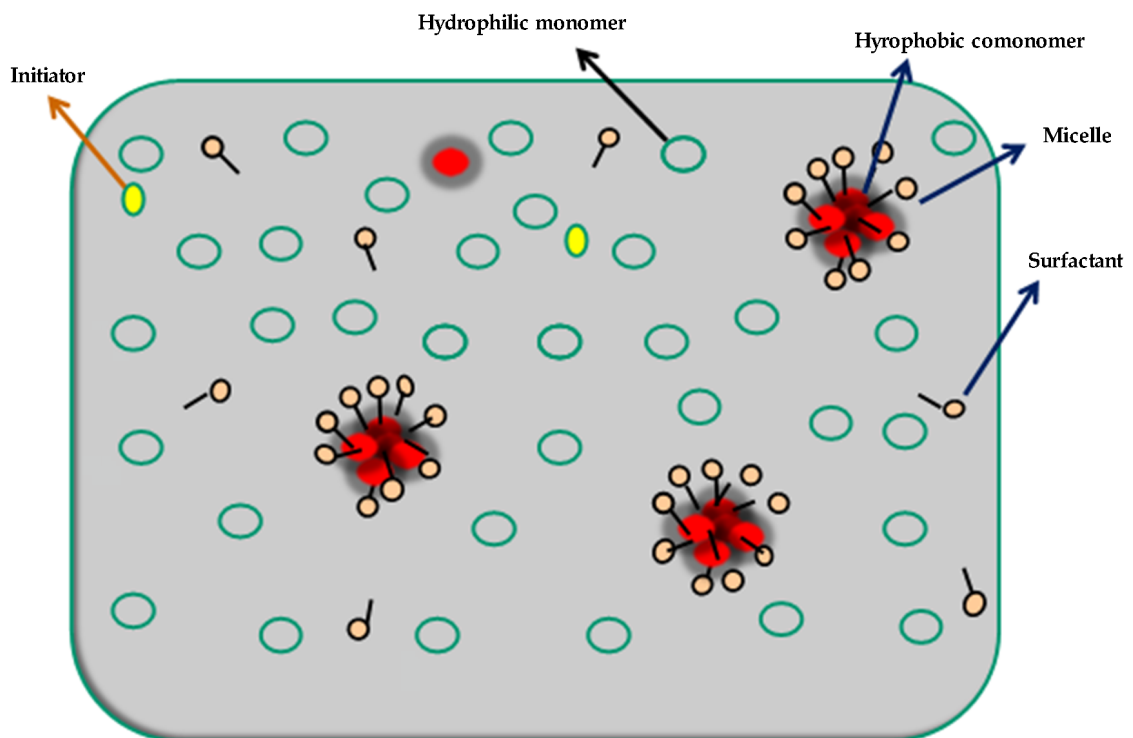


**Figure 8.** Scheme showing micellar copolymerization of hydrophilic and hydrophobic monomers via free-radical mechanism in aqueous surfactant solution.

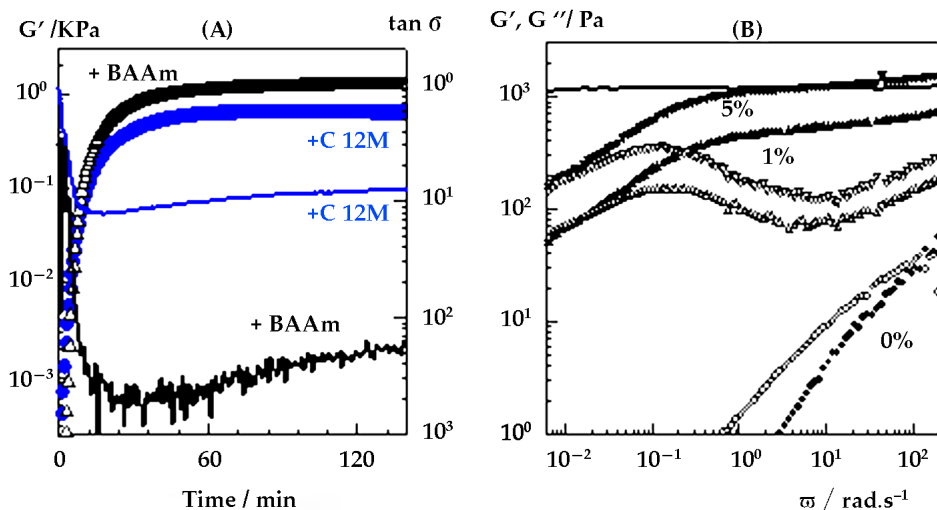


**Figure 9.** Reaction time dependent variations of  $G'$  (symbols) and  $\tan \delta$  (lines) during the micellar copolymerization of 5 w/v% AAm with 1 mol% C12 (blue), and 1 mol% BAAm (black).  $\omega = 6.28$  rad/s.  $\gamma_0 = 0.01$ . (B):  $G'$  (filled symbols) and  $G''$  (open symbols) of 5 w/v% PAAm in SDS (aq) with 0 (circles), 1 (triangles up) and 5 mol% C12M (triangles down) shown as a function of the frequency  $\omega$ . For comparison,  $G'$  versus  $\omega$  plot of PAAm gel formed using 1 mol% BAAm is also shown by the solid curve.  $\gamma_0 = 0.01$ . SDS = 7 w/v%. From [51] with permission from Elsevier.

rimental time scale [51]. Because of these reversible cross-links, C12M-containing hydrogels exhibited autonomous self-healing at room temperature while the chemically cross-linked ones could not be healed.

Hydrophobically modified hydrogels exhibit time dependent viscoelastic properties due to their physical cross-links. Figure 9B presents a typical example where the dynamic moduli of physical PAAm hydrogels with 1 and 5 mol% C12M are shown as a function of frequency  $\omega$  [51]. For comparison, the data for PAAm solutions prepared in the absence of C12M are also shown in the figure. They all were prepared under the same experimental condition at a total monomer concentration of 5 w/v%. In the absence of C12M, the system exhibits a liquid-like response with a crossover frequency of  $10^2$  rad/s, as typical for a semi-dilute polymer solution. Incorporation of C12M segments into the PAAm chains shifts the crossover frequency to  $10^{-2}$  rad/s revealing 4 orders of magnitude increase in the effective relaxation time of the gel network. Since this relaxation time relates to the average time during which a polymer chain disentangles from an entanglement point, the result indicates formation of strong and long lived associations between the blocks of dodecyl groups in the semi-di-

lute solution [51]. The effect of alkyl side chain length of *n*-alkyl acrylamides on the hydrogel properties was also investigated in detail [50]. The longer the alkyl chain length, the higher is both  $G''$  and  $G'$  of the resulting hydrophobically modified hydrogels at high frequencies. The results also show that the lifetime of hydrophobic associations increases with increasing side chain length of the hydrophobic monomers [50].

However, larger hydrophobes with a side chain length larger than 12 carbon atoms were insoluble in the micellar solutions of SDS, which hindered their micellar copolymerization with hydrophilic monomers. This insolubility of large hydrophobes is due to their larger sizes as compared to the size of the micelles. To overcome this limitation, wormlike micelles (WLMs) having a large solubilization power for hydrophobes were used during the micellar polymerization [37,52-54]. WLMs were produced by adding salts in aqueous SDS solutions; this weakens electrostatic interactions and causes the micelles to grow, which, in turn, provides solubilization of a large amount of hydrophobes in the micellar solution. For instance, the solubility of C18A monomer in a micellar solution increases from 0 to 16 w/v% as NaCl concentration increases from 0 to 1.5 M [37].

Figure 10A shows viscoelastic properties of hydrophobically modified hydrogels formed by micellar copolymerization of AAm with 2 mol% of various hydrophobic monomers with long alkyl side chains in SDS-NaCl solution [53]. The hydrophobic monomers are abbreviated as CxR, where C stands for carbon, x is the number of carbon atoms in side alkyl chain, and R equals to A or M for acrylates and methacrylates, respectively. Note that C17.3M represents the commercially available stearyl methacrylate composed of 65% n-octadecyl methacrylate and 35% n-hexadecyl methacrylate. All hydrogels show time-dependent storage  $G'$  and loss moduli  $G''$  with a plateau in  $G'$  at frequencies above  $>10^2$  rad/s, indicating the temporary nature of the hydrophobic associations with lifetimes of the order of seconds to milliseconds [53]. The physical gel formed using C22A exhibits a much slower relaxation at low frequencies compared to other hydrophobes, which is due to the increasing activation energy for disengagement of hydrophobic blocks with increasing length of alkyl side chains. The

plateau in  $G'$  at frequencies above  $>10^2$  rad/s, indicating the temporary nature of the hydrophobic associations with lifetimes of the order of seconds to milliseconds [53]. The physical gel formed using C22A exhibits a much slower relaxation at low frequencies compared to other hydrophobes, which is due to the increasing activation energy for disengagement of hydrophobic blocks with increasing length of alkyl side chains. The

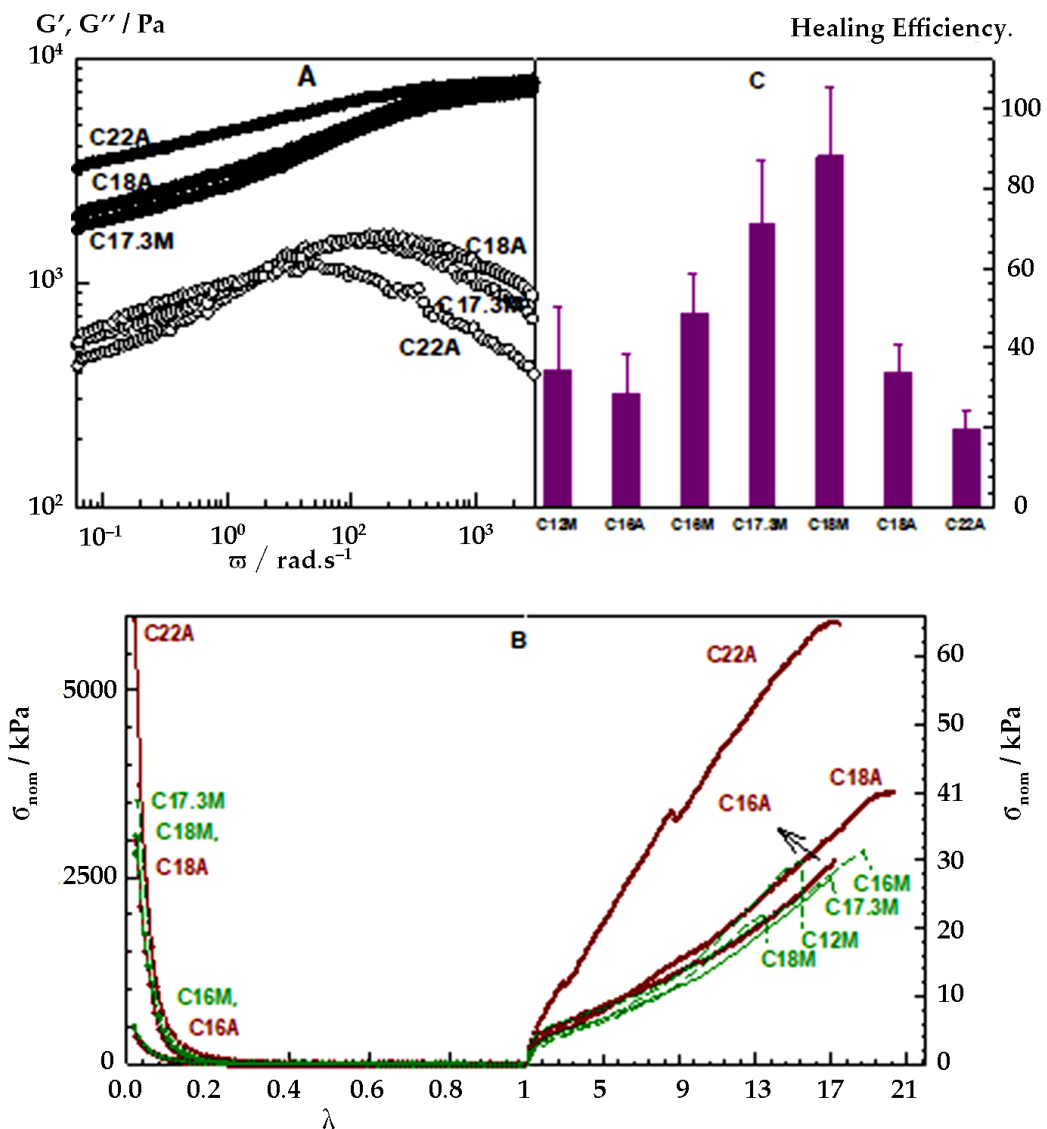


**Figure 10.** (A):  $G'$  (filled symbols) and  $G''$  (open symbols) of hydrophobically modified PAAm hydrogels shown as a function of  $\omega$ .  $\nu_0 = 0.01$ . Type of the hydrophobes indicated. (B): Stress-strain curves of the hydrogels under compression and elongation as the dependence of nominal stress  $\sigma_{\text{nom}}$  on the deformation ratio  $\lambda$ . (C): Healing efficiency for the gels formed using 7 different hydrophobes. From [53] with permission from Elsevier.

viscoelastic behavior of the hydrogels was also reflected in their mechanical properties [53]. Figure 10B shows stress-strain curves of hydrophobically modified hydrogels containing 2 mol% hydrophobic units with various alkyl side chain lengths. In compression tests ( $\lambda < 1$ ), all hydrogels are stable up to a compression ratio of 96%. In elongation tests,  $\lambda$  at break is larger than 16, i.e., the elongation exceeds 1500% for all the physical hydrogels while the ultimate strength of the hydrogels formed using hydrophobic acrylates is larger than those formed using methacrylates (30–65 vs. 20–30 kPa) [53]. Due to the reversible nature of cross-links in hydrophobically modified hydrogels, they all exhibited self-healing behavior. To quantify the efficiency of self-healing, cut-and-heal tests were carried out at 25°C for 30 min. Figure 10C shows the healing efficiencies of the hydrogels with respect to the elongation ratio at break of the virgin ones [53]. Two important results are seen from the figure:

1) The healing efficiency increases as the length of the alkyl side chain increases up to 18 carbon atoms but then decreases again. C18M hydrophobe provides the maximum healing efficiency of around 80%. Thus, self-healing ability critically depends on the length of side alkyl chains of the hydrophobic monomers.

2) Hydrophobic methacrylates produces hydrogels with a higher healing efficiency as compared to the corresponding acrylates. For instance, by replacing C18A with C18M, or C16A with C16M, the efficiency of healing increases from 34 to 88%, and from 29 to 49%, respectively [53]. This finding indicates the effect of the backbone methyl group on the self-healing efficiency of the hydrogels, which is likely due to the limited flexibility of the methacrylate backbones as compared to the acrylate ones.

It was shown that not only the type and side chain length of the hydrophobic monomer, but also the type of the hydrophilic monomer determines the healing efficiencies of hydrophobically modified hydrogels. A series of hydrophobically modified hydrogels were prepared in aqueous WLMs by copolymerization of hydrophilic monomers DMAA, NIPAM, and AAm with 2 mol% C17.3M [52,55,56]. The highest stretchability was obtained when DMAA is used in the hydrogel preparation (4200±400%) [55], which is likely due to its associative property (Figure 11A). Moreover, cyclic mechanical tests conducted up to a maximum strain below failure

revealed that PDMAA hydrogels exhibit a significant hysteresis behavior [55]. The hysteresis was quantified by the hysteresis energy  $U_{hys}$ , which is the area surrounded by the loading and unloading curves.  $U_{hys}$  corresponds to the amount of dissipated energy, i.e., the number of intermolecular bonds broken under stress. Figure 11B shows that  $U_{hys}$  increases with increasing maximum strain, independent of the type of strain. Moreover, when the cyclic mechanical tests are repeated several times on the same gel specimen, all the cycles overlapped indicating of reformation (healing) of the broken bonds. Calculations show that around half of the intermolecular physical cross-links are broken reversibly at an elongation ratio of 20 (Figure 11C) [55]. This reveals reversible dissociation of the hydrophobic associations under an external stress and thus point out the self-healing ability of hydrophobically modified hydrogels.

The images in Figure 12A show a hydrophobically modified PDMAA hydrogel specimen before and after elongation up to  $\lambda = 10$  [55]. The stretched physical hydrogel returns to its initial length within 10 min demonstrating the recovery of the virgin shape. Moreover, when the same hydrogel is first cut into two parts and then healed by bringing the cut surfaces together, the healed specimen withstands very large elongation ratios before its fracture (Figure 12B). Figure 11D shows stress-strain curves of hydrogel samples that were first cut into two parts and then healed at 24°C for different healing times. The curve of the virgin hydrogel is also shown in the figure. It is seen that a complete healing could be achieved within for 20 min [55]. Self-healing mechanism in hydrophobically modified hydrogels containing surfactant micelles was recently explained by time dependent monitoring of the cut surfaces using scanning force microscopy [54]. It was shown that the healing process starts with a fast step and then proceeds slowly towards a complete healing. During the first step, the trenches and protrusions on the surface of the damaged hydrogel change in shape to become round holes and islands during which their height and depth remain unchanged (a and b in Figure 13A). We can explain this first step with the formation of hydrophobic associations between hydrophobes locating nearby at the damaged surface, i.e., at the edge of the trenches so that they transform to a circular shape. During the second slow step, the islands and holes on the gel surface gradually disappear and the virgin gel surface is recovered (c in Figure 13A). This step requires diffusion of hydrophobes along the gel surface and hence requires a longer time as compared to the first step.

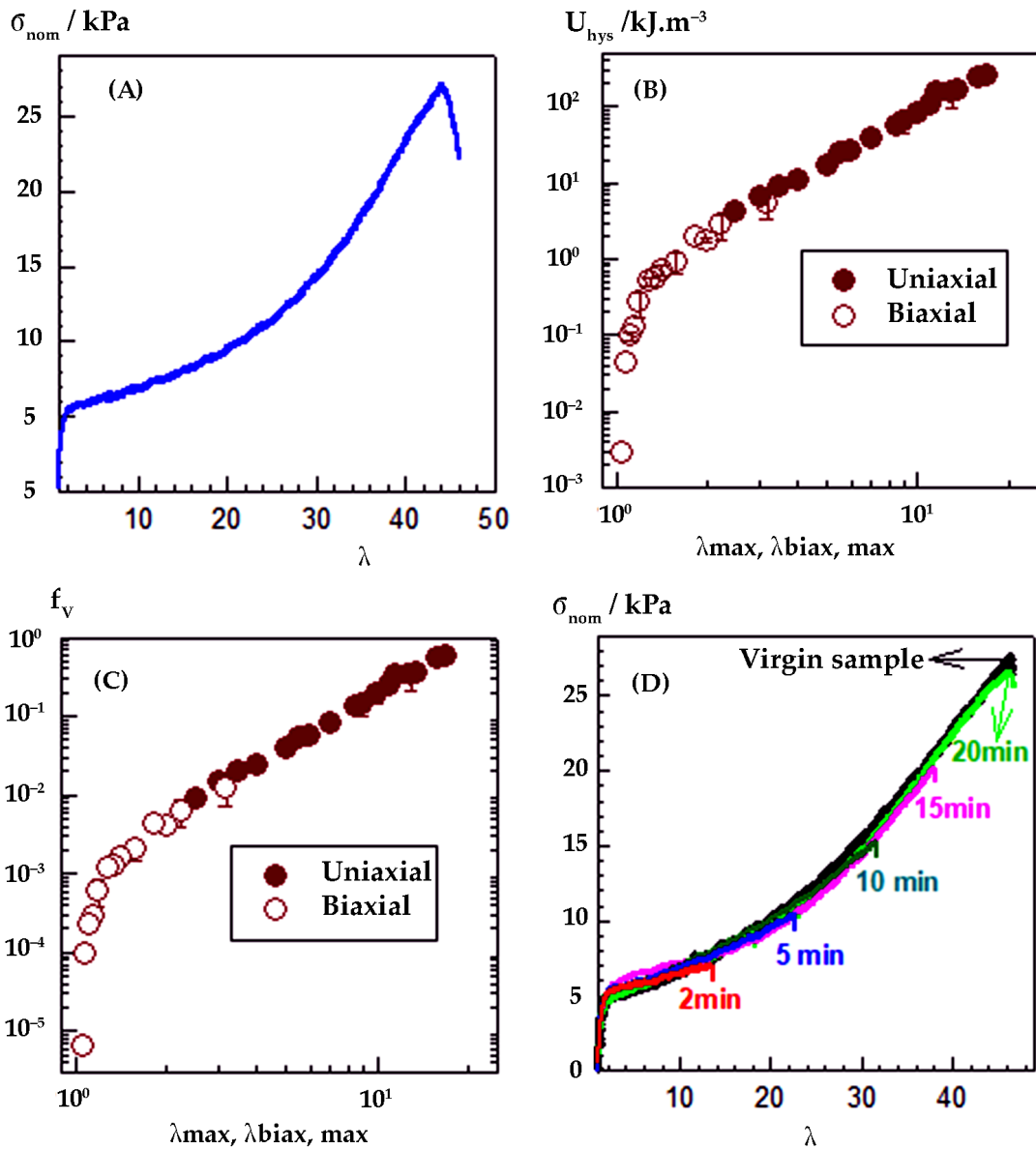


**Figure 11.** (A): Stress-strain curve of PDMAA hydrogel under elongation. DMAA = 10 w/v%. C17.3M = 2 mol% with respect to DMAA. (B, C): Hysteresis energy  $U_{hys}$  (B) and the fraction  $f_v$  of dissociated cross-links (C) during the loading/unloading compression (open symbols) and elongation cycles (filled symbols) of PDMAA hydrogels shown as a function of the maximum strain ( $\lambda_{max}$  and  $\lambda_{biax, max}$ ). (D): Stress-strain curves of healed hydrogels at various healing times as indicated. From [55] with permission from Elsevier.

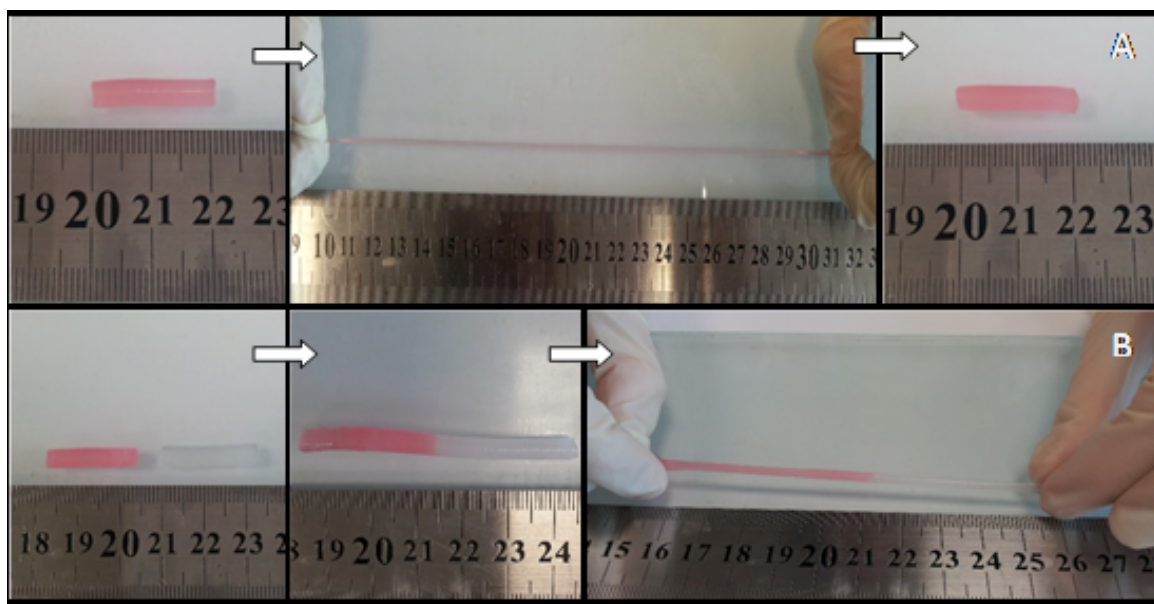


**Figure 12.** (A): Photographs of a hydrogel before and after stretching to an elongation ratio of 10, and after recovery its original length within 10 min. (B): Photographs of two gel samples after cutting into two pieces, after healing by pushing the cut surfaces together for 10 min. One of the gels was colored for clarity. From [55] with permission from Elsevier.

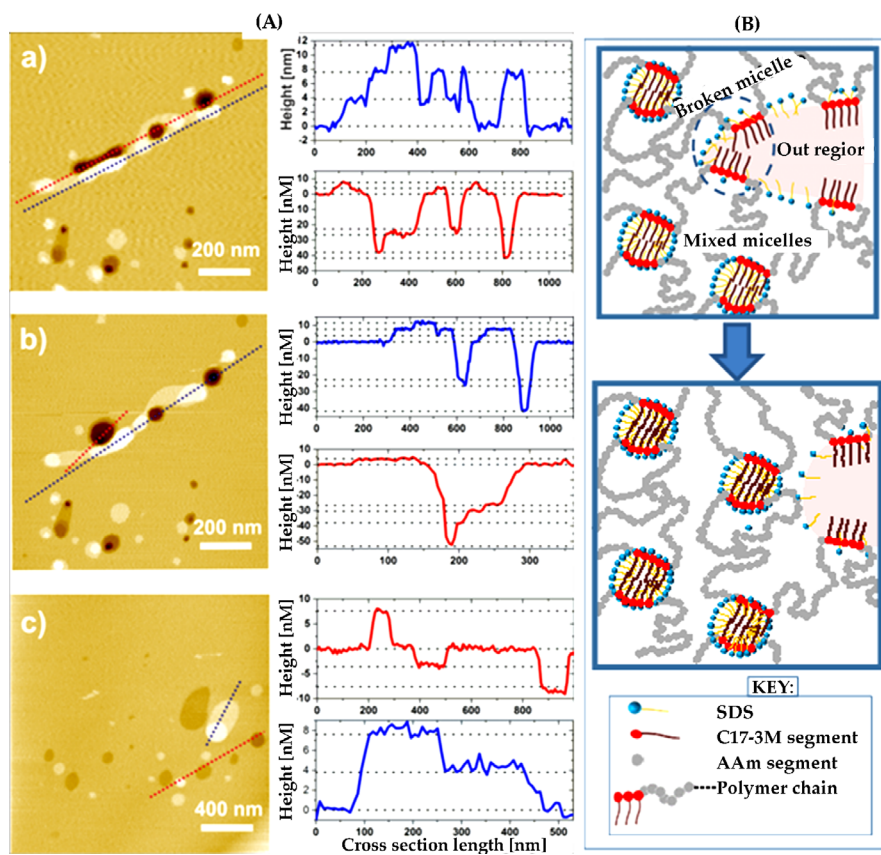


**Figure 13.** (A): Topography images of gel surface just after cutting the surface (a), after a few tens of seconds (b); and after 75 min (c). The colored dotted lines across the images indicate the cross sections on the right side of the images in the respective colors. The color scale of the images is 50 nm from black to white. (B): Cartoon showing self-healing mechanism of hydrophobically modified hydrogels containing surfactant micelles. From [54] with permission from the American Chemical Society.

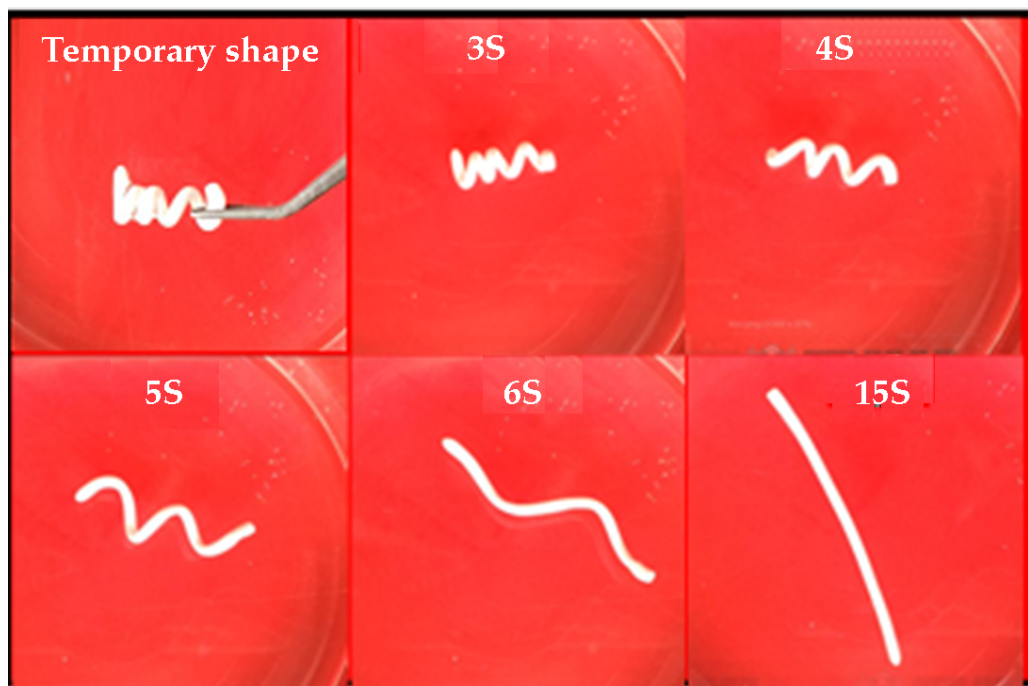


**Figure 14.** (A): Images demonstrating the transition from the temporary spiral shape to the permanent rod shape for a PAAc hydrogel with 50% C18A. From [37] with permission from the American Chemical Society.

### 3. Self-healing and shape-memory hydrogels

Shape-memory hydrogels (SMHs) typically consist of a 3D network structure formed by permanent and temporary cross-links, denoted as the netpoints and switching segments, respectively [36,37]. Chemical cross-links are generally used as the netpoints to determine the permanent shape, while glassy or crystalline domains serve as the switching segments for fixing the temporary shape of SMHs. The images in Figure 14 shows typical shape-memory behavior of a hydrogel containing both chemical cross-links and crystalline domains with a melting temperature  $T_m$  of  $48 \pm 2^\circ\text{C}$  [37]. The permanent shape of the specimen is rod. When heated above  $T_m$ , it becomes soft so that it can easily be deformed to a spiral shape. This temporary shape was fixed by cooling the specimen below  $T_m$  during which crystalline domains reform and lock the deformed chain conformation. By heating the sample above  $T_m$ , it returns to its initial shape within 20 s. The chemically cross-linked network structure of the hydrogel determines the permanent rod shape while crystalline domains serving as the switching segments fix the temporary spiral shape. The principle of

thermos-responsive shape memory behavior is that the covalently cross-linked network structure restores its random coil conformation when the temperature is elevated above  $T_m$  of crystalline domains.

Preparation of hydrogels with both self-healing and shape memory functions requires a physical hydrogel network containing strong and weak cross-links acting as the netpoints and switching segments, respectively. Such hydrogels were prepared on the basis of complex formation between hydrophobically modified polyacrylic acid (PAAc) and cetyltrimethylammonium (CTA) counterions [57]. The hydrogels exhibit a tensile strength of 1.7 MPa and shape-memory behavior due to the significant variation of their moduli with temperature. However, the shape fixity ratio of the hydrogels was low due to the non-crystalline state of the hydrophobic segments that cannot support the residual stress in PAAc chains [57].

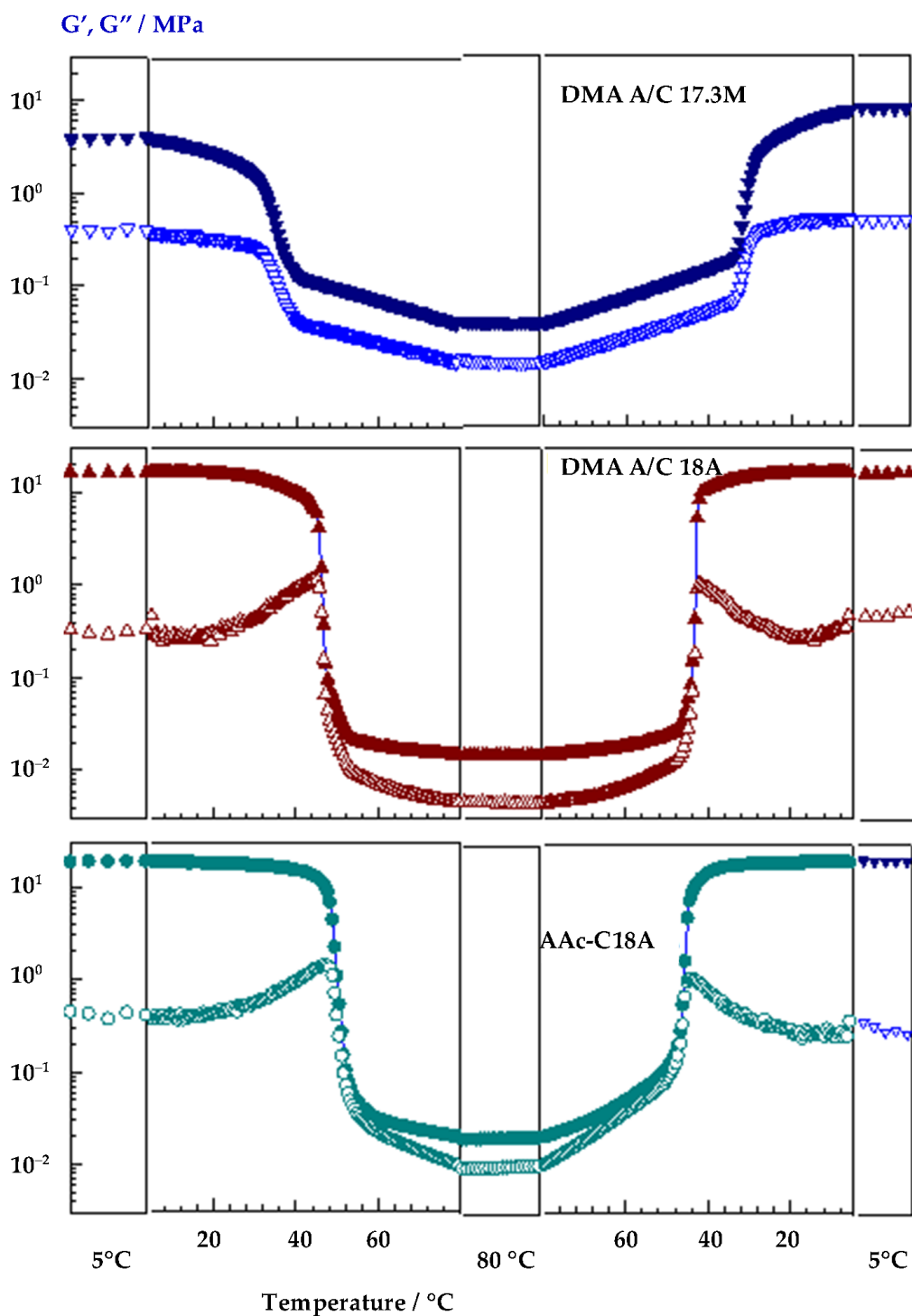


**Figure 15.**  $G'$  (filled symbols), and  $G''$  (open symbols) of the hydrogels during the heating - cooling cycle between 80 and 5°C. The type of the hydrogels indicated. Hydrophobe content = 50 mol%.  $\omega = 6.28 \text{ rad/s}$ .  $\gamma_0 = 0.1\%$ . From [20] with permission from Elsevier.

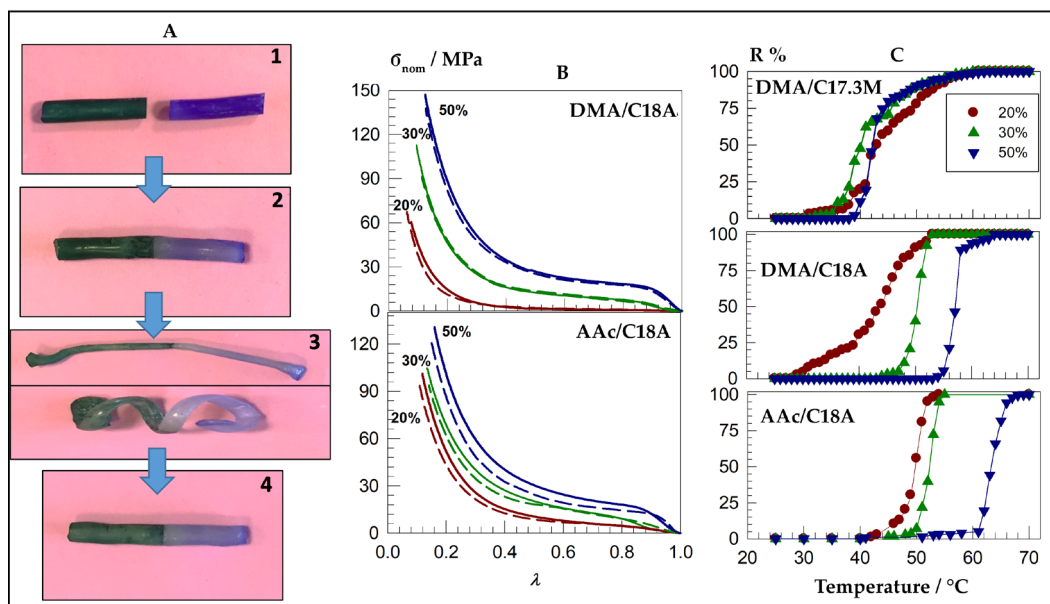


**Figure 15.** (A) Images demonstrating self-healing and shape-memory functions of hydrophobically modified PAAc hydrogels. They were colored for clarity. After pushing the cut surfaces together at 80°C for 24 h, they merge into a single piece (2). The healed hydrogel can be transformed into any temporary shape by first heating to 70°C, and then cooling to room temperature (3). The recovery of the original shape occurs by heating again to 70°C (4). (B) Stress-strain curves of virgin and healed hydrogel samples shown by the solid and dashed curves, respectively. (C) Temperature dependence of the shape recovery ratio  $R$  of the hydrogels. From [20] with permission from Elsevier.

A simple and versatile strategy to prepare self-healing and shape-memory hydrogels is bulk photopolymerization of hydrophilic and hydrophobic monomers leading to hydrogels containing hydrophobic associations and crystalline domains [20]. The hydrogels were prepared by bulk copolymerization of the hydrophilic monomers DMAA or AAc with the hydrophobic monomers C17.3M, and C18A. The mole fraction of the hydrophobic monomer in the feed was between 0.2 and 0.5. The copolymerization reactions initiated using Irgacure 2959 initiator under UV light resulted in the formation of semi-crystalline polymers. After swelling in water, hydrogels with water contents between 7 and 56% were obtained. The melting temperature  $T_m$  and the degree of crystallinity were between 36–56°C and 3–33%, and they increased with increasing hydrophobic monomer content, or by replacing C17.3M units with C18A ones [20].

The flexibility of hydrophilic PDMAA and PAAc network chains in water provides alignment of the hydrophobic units to form crystalline regions. The hydrogels exhibit 120- to 1000-fold change in the modulus by changing the temperature between below and above  $T_m$  (Figure 15) [20]. This significant modulus variation depending

on temperature provides effective self-healing and shape-memory functions to the hydrogels. Figure 16A represents these functions of two DMAA/AAc hydrogel specimens with 30 mol% hydrophobe [20]. After pressing their cut surfaces together above  $T_m$ , they merge into a single piece (2). When cooled below  $T_m$ , the healed hydrogel specimen recovers its original mechanical performances, as shown by the stress-strain curves of virgin and healed specimens in Figure 16B. Moreover, when the healed gel sample is again heated above  $T_m$ , it becomes soft so that any temporary shape can be given which is then fixed by cooling the sample to 24°C (3). By heating the gel sample in a water bath at 70°C, it returns to its initial shape within 15 s (4). Figure 16C shows the shape recovery ratio  $R$  of the hydrogels plotted as a function of temperature. The shape-recovery ratio at or above 52°C is 100% for all hydrogels. The results indicate that the hydrophobic units forming hydrophobic associations act as physical crosslinks, i.e., as netpoints to restore the random coil conformation of the deformed network chains. Below  $T_m$ , they form crystalline domains and thus act as switching segments to fix the temporary shape.

#### 4. Conclusions

Hydrogels are unique materials with a wide range of applications due to their softness, stimuli-responsiveness, and great similarity to biological systems. The classical first-generation hydrogels were generally brittle in nature which limited their load-bearing applications. The second generation hydrogels developed in the past decade show extraordinary mechanical performances similar to those of load-bearing tissues such as tendons, cartilage, and ligaments. Designing self-healing and shape-memory functions in soft materials is another challenge in the last years. Here recent developments in the field of self-healing and shape-memory hydrogels formed via non-covalent interactions are presented by focusing on H-bonding and hydrophobic interactions.

Preparation of self-healing hydrogels via H-bonds that are stable in water requires multiple H-bonding interactions between polymer chains. Monomers such as NAGA carrying dual amide groups, DAT and UPy groups forming multiple H-bonds can be used to produce mechanically strong H-bonded hydrogels with self-healing ability. Another simple alternative is the copolymerization of vinyl monomers with H-bond acceptor and donor sites such as DMAA/MAAc, and DMAA/AMPS comonomer pairs in aqueous solutions. Self-healing hydrogels via hydrophobic associations have generally been prepared by micellar copolymerization of hydrophilic and hydrophobic monomers in aqueous solutions of monomeric or wormlike micelles. The mechanical strength of hydrophobically modified hydrogels increases with increasing hydrophobe content, with increasing length of side alkyl chains, or with increasing primary chain length of the physical network. Preparation of hydrogels with both self-healing and shape-memory functions requires a physical hydrogel network containing strong and weak cross-links. They can easily be prepared by bulk photopolymerization of hydrophilic monomers such as DMAA or AAc with 20-50 mol% hydrophobic monomers C17.3M or C18A. In these hydrogels, the hydrophobic units form hydrophobic associations and crystalline domains acting as netpoints switching segments, respectively.

**Acknowledgments** – The author thanks the Turkish Academy of Sciences (TUBA) for the partial support.

#### References

- O. Okay, General properties of hydrogels. in G. Gerlach and K.-F. Arndt, eds., *Hydrogel sensors and actuators*, Springer Series on Chemical Sensors and Biosensors, 6 (2009) 1-14.
- Y. Tanaka, J.P. Gong, Y. Osada, Novel hydrogels with excellent mechanical performance, *Prog. Polym. Sci.*, 30 (2005) 1-9.
- P. Calvert, Hydrogels for soft machines, *Adv. Mater.*, 21 (2009) 743-756.
- O. Wichterle, D. Lim, Hydrophilic gels for biological use, *Nature*, 185 (1960) 117-118.
- T. Tanaka, Collapse of gels and the critical endpoint, *Phys. Rev. Lett.*, 40 (1978) 820-823.
- H. Staudinger, E. Husemann, Über hochpolymere Verbindungen, 116. Über das begrenzt quellbare Polystyrol. *Ber. Dtsch. Chem. Ges.* 68 (1935) 1618-1634.
- H.R. Brown, A model of the fracture of double network gels, *Macromolecules*, 40 (2007) 3815-3818.
- A. Ahagon, A.N. Gent, Threshold fracture energies for elastomers, *J. Polym. Sci. Polym. Phys. Ed.*, 12 (1975) 1903-1911.
- C. Creton, 50th Anniversary perspective: Networks and gels: Soft but dynamic and tough, *Macromolecules*, 50 (2017) 8297-8316.
- J.P. Gong, Why are double network hydrogels so tough?, *Soft Matter*, 6 (2010) 2583-2590.
- X. Zhao, Multi-scale multi-mechanism design of tough hydrogels: building dissipation into stretchy networks, *Soft Matter*, 10 (2014) 672-687.
- J.P. Gong, Y. Katsuyama, T. Kurokawa, Y. Osada, Double-network hydrogels with extremely high mechanical strength, *Adv. Mater.*, 15 (2003) 1155-1158.
- Q. Chen, D. Wei, H. Chen, L. Zhu, C. Jiao, G. Liu, L. Huang, J. Yang, L. Wang, J. Zheng, Simultaneous enhancement of stiffness and toughness in hybrid double-network hydrogels via the first, physically linked network, *Macromolecules*, 48 (2015) 8003-8010.
- J. Li, Z. Suo, J.J. Vlassak, Stiff, strong, and tough hydrogels with good chemical stability, *J. Mater. Chem. B*, 2 (2014) 6708-6713.
- J.-Y. Sun, X. Zhao, W.R.K. Illeperuma, O. Chaudhuri, K.H. Oh, D.J. Mooney, J.J. Vlassak, Z. Suo, Highly stretchable and tough hydrogels, *Nature*, 489 (2012) 133-136.
- L. Zhang, J. Zhao, J. Zhu, C. He, H. Wang, Anisotropic tough poly(vinyl alcohol) hydrogels, *Soft Matter*, 8 (2012) 10439-10447.
- K. Haraguchi, T. Takehisa, Nanocomposite hydrogels: a unique organic-inorganic network structure with extraordinary mechanical, optical, and swelling/de-swelling properties, *Adv. Mater.*, 14 (2002) 1120-1124.
- T.L. Sun, T. Kurokawa, S. Kuroda, A.B. Ihsan, T. Akasaki, K. Sato, M.A. Haque, T. Nakajima, J.P. Gong, Physical hydrogels composed of polyampholytes demonstrate high toughness and viscoelasticity, *Nat. Mater.*, 12 (2013) 932-937.
- X. Hu, M. Vatankehah-Varnoosfaderani, J. Zhou, Q. Li, S.S. Sheiko, Weak hydrogen bonding enables hard, strong, tough, and elastic hydrogels, *Adv. Mater.*, 27 (2015) 6899-6905.
- B. Kurt, U. Gülyüz, D.D. Demir, O. Okay, High-strength semi-crystalline hydrogels with self-healing and shape memory functions., *Eur. Polym. J.*, 81 (2016) 12-23.
- C. Bilici, S. Ide, O. Okay, Yielding behavior of tough semicrystalline hydrogels, *Macromolecules*, 50 (2017) 3647-3654.

22. M.D. Hager, S. van der Zwaag, U.S. Schubert (eds) (2016) Self-healing Materials. *Adv. Polym. Sci.* 273 (2016) 413 pp
23. D.L. Taylor, M. in het Panhuis, Self-healing hydrogels, *Adv. Mater.*, 28 (2016) 9060-9093.
24. O. Okay, Self-healing hydrogels formed via hydrophobic interactions, *Adv. Polym. Sci.*, 268 (2015) 101-142.
25. O. Okay, Semicrystalline physical hydrogels with shape-memory and self-healing properties, *J. Mater. Chem. B*, 7 (2019) 1581-1596.
26. C. Creton, O. Okay (eds) (2020) Self-healing and self-recovering hydrogels. *Adv. Polym. Sci.* 285, 388 pp.
27. S. Talebian, M. Mehrali, N. Taebnia, C.P. Pennisi, F.B. Kadumudi, J. Foroughi, M. Hasany, M. Nikkiah, M. Akbari, G. Orive, A. Dolatshahi-Pirouz, Self-healing hydrogels: the next paradigm shift in tissue engineering?, *Adv. Sci.*, 6 (2019) 1801664.
28. Q. Li, C. Liu, J. Wen, Y. Wu, Y. Shan, J. Liao, The design, mechanism and biomedical application of self-healing hydrogels, *Chin. Chem. Lett.*, 28 (2017) 1857-1874.
29. S. Strandman, X.X. Zhu, Self-healing supramolecular hydrogels based on reversible physical interactions, *Gels*, 2 (2016) 16 1-31.
30. W. Wang, Y. Zhang, W. Liu, Bioinspired fabrication of high strength hydrogels from non-covalent interactions, *Prog. Polym. Sci.*, 71 (2017) 1-25.
31. A. Lendlein, S. Kelch, Shape-memory polymers, *Angew. Chem. Int. Ed.*, 41 (2002) 2034-2057.
32. C. Liu, H. Qin, P.T. Mather, Review of progress in shape-memory polymers, *J. Mater. Chem.*, 17 (2007) 1543-1558.
33. M. Behl, M.Y. Razzaq, A. Lendlein, Multifunctional shape-memory polymers, *Adv. Mater.*, 22 (2010) 3388-3410.
34. Y. Osada, A. Matsuda, Shape memory in hydrogels, *Nature*, 376 (1995) 219.
35. B. Gyarmati, B.A. Szilágyi, A. Szilágyi, Reversible interactions in self-healing and shape memory hydrogels, *Eur. Polym. J.*, 93 (2017) 642-669.
36. U. Nöchel, C.S. Reddy, N.K. Uttamchand, K. Kratz, M. Behl, A. Lendlein, Shape-memory properties of hydrogels having a poly( $\epsilon$ -caprolactone) crosslinker and switching segment in an aqueous environment, *Eur. Polym. J.*, 49 (2013) 2457-2466.
37. C. Bilici, O. Okay, Shape memory hydrogels via micellar copolymerization of acrylic acid and n-octadecyl acrylate in aqueous media, *Macromolecules*, 46 (2013) 3125-3131.
38. C. Bilici, V. Can, U. Nöchel, M. Behl, A. Lendlein, O. Okay, Melt-processable shape-memory hydrogels with self-healing ability of high mechanical strength, *Macromolecules*, 49 (2016) 7442-7449.
39. J. Hao, R.A. Weiss, Mechanically tough, thermally activated shape memory hydrogels, *ACS Macro Lett.*, 2 (2013) 86-89.
40. X. Dai, Y. Zhang, L. Gao, T. Bai, W. Wang, Y. Cui, W. Liu, A mechanically strong, highly stable, thermoplastic, and self-healable supramolecular polymer hydrogel, *Adv. Mater.*, 27 (2015) 3566-3571.
41. K.E. Maly, C. Dauphin, J.D. Wuest, Self-assembly of columnar mesophases from diaminotriazines, *J. Mater. Chem.*, 16 (2006) 4695-4700.
42. B. Liu, W. Liu, Poly(vinyl diaminotriazine): from molecular recognition to high-strength hydrogels, *Macromol. Rapid Commun.*, 39 (2018) 1800190.
43. M. Guo, L.M. Pitet, H.M. Wyss, M. Vos, P.Y.W. Dankers, E.W. Meijer, Tough stimuli-responsive supramolecular hydrogels with hydrogen-bonding network junctions, *J. Am. Chem. Soc.*, 136 (2014) 6969-6977.
44. H. Ding, X.N. Zhang, S.Y. Zheng, Y. Song, Z.L. Wu, Q. Zheng, Hydrogen bond reinforced poly(1-vinylimidazole-co-acrylic acid) hydrogels with high toughness, fast self-recovery, and dual pH responsiveness, *Polymer*, 131 (2017) 95-103.
45. X.N. Zhang, Y.J. Wang, S. Sun, L. Hou, P. Wu, Z.L. Wu, Q. Zheng, A tough and stiff hydrogel with tunable water content and mechanical properties based on the synergistic effect of hydrogen bonding and hydrophobic interaction, *Macromolecules*, 51 (2018) 8136-8146.
46. G. Song, L. Zhang, C. He, D.-C. Fang, P.G. Whitten, H. Wang, Facile fabrication of tough hydrogels physically cross-linked by strong cooperative hydrogen bonding, *Macromolecules*, 46 (2013) 7423-7435.
47. E. Su, O. Okay, A self-healing and highly stretchable polyelectrolyte hydrogel via cooperative hydrogen-bonding as a superabsorbent polymer, *Macromolecules*, 52 (2019) 3257-3267.
48. A.T. Üzümcü, O. Güney, O. Okay, Highly stretchable DNA/clay hydrogels with self-healing ability, *ACS Appl. Mater. Interfaces*, 10 (2018) 8296-8306.
49. A. Hill, F. Candau, J. Selb, Properties of hydrophobically associating polyacrylamides: influence of the method of synthesis, *Macromolecules*, 26 (1993) 4521-4532.
50. S. Abdurrahmanoglu, V. Can, O. Okay, Design of high-toughness polyacrylamide hydrogels by hydrophobic modification, *Polymer*, 50 (2009) 5449-5455.
51. S. Abdurrahmanoğlu, M. Çilingir, O. Okay, Dodecyl methacrylate as a crosslinker in the preparation of tough polyacrylamide hydrogels, *Polymer*, 52 (2011) 694-699.
52. D.C. Tuncaboğlu, M. Şahin, A. Argun, W. Oppermann, O. Okay, Dynamics and large strain behavior of self-healing hydrogels with and without surfactants, *Macromolecules*, 45 (2012) 1991-2000.
53. D.C. Tuncaboğlu, A. Argun, M. Şahin, M. Sari, O. Okay, Structure optimization of self-healing hydrogels formed via hydrophobic interactions, *Polymer*, 53 (2012) 5513-5522.
54. V. Can, Z. Kochovski, V. Reiter, N. Severin, M. Siebenbürger, B. Kent, J. Just, J.P. Rabe, M. Ballauff, O. Okay, Nanostructural evolution and self-healing mechanism of micellar hydrogels, *Macromolecules*, 49 (2016) 2281-2287.
55. M.P. Algi, O. Okay, Highly stretchable self-healing poly(N,N-dimethylacrylamide) hydrogels, *Eur. Polym. J.*, 59 (2014) 113-121.
56. U. Gülyüz, O. Okay, Self-healing poly(N-isopropylacrylamide) hydrogels, *Eur. Polym. J.*, 72 (2015) 12-22.
57. U. Gülyüz, O. Okay, Self-healing poly(acrylic acid) hydrogels with shape memory behavior of high mechanical strength, *Macromolecules*, 47 (2014) 6889-6899.